Diffuse phase transitions in ferroelectric ultrathin films from first principles

S. Bin-Omran,[1] I. Kornev,[2] I. Ponomareva,[3] and L. Bellaiche[4]
[1]*Department of Physics and Astronomy, King Saud University, Riyadh 11451, Saudi Arabia*
[2]*Laboratoire SPMS, UMR 8580 du CNRS, Ecole Centrale Paris, 92295 Chatenay-Malabry, France*
[3]*Department of Physics, University of South Florida, Tampa, Florida 33620, USA*
[4]*Physics Department, University of Arkansas, Fayetteville, Arkansas 72701, USA*
(Received 22 December 2009; revised manuscript received 16 February 2010; published 30 March 2010)

A first-principles-derived scheme is developed and used to investigate the diffuse character of the paraelectric-to-ferroelectric transition in ultrathin films made of $BaTiO_3$, and to reveal its dependency on mechanical and electrical boundary conditions, as well as on thickness. It is found that such diffuse character does not require the presence of defects to occur, unlike commonly believed, but rather can originate from surface-induced dipolar inhomogeneities in defect-free films.

DOI: 10.1103/PhysRevB.81.094119 PACS number(s): 77.80.B−, 77.22.Ch, 77.22.Ej

I. INTRODUCTION

Ferroelectric (FE) thin films are of considerable technological interest because of their potential in nonvolatile memories, communication devices, and nanoelectromechanical systems.[1–4] Intense effort has been made recently to determine if properties of these low-dimensional systems can differ from those of the corresponding bulk. As a result, it has been discovered that characteristics of thin films—that are, the film's thickness, the strain arising from the substrate and the depolarizing field originating from the incomplete screening of the polarization-induced charges at the surfaces/interfaces—can generate novel properties of fundamental and technological interest. For instance, a minimal critical thickness below which a single ferroelectric monodomain disappears was predicted to occur in FE thin films,[5] and epitaxial conditions were found to induce structural phases that do not exist in the corresponding bulk (see, e.g., Refs. 6 and 7, and references therein). Similarly, novel complex dipolar patterns (such as ferroelectric stripes and bubbles) were discovered to form and to originate from the depolarizing field existing inside these films.[8–10] One remaining important "mystery" in FE thin films concerns the reported *diffuse* character of their paraelectric-to-ferroelectric transition[11–21] (a diffuse phase transition is characterized by a smearing of the phase transition in a rather wide temperature interval around the temperature at which the dielectric constant reaches its maximum,[22] which makes it technologically promising for designing devices efficiently operating in a large temperature range). As a matter of fact, the microscopic origins of this diffuseness, and why such diffuseness has been observed to be enhanced when increasing the magnitude of the epitaxial strain[11,12] or when decreasing the film thickness,[13–15] are poorly known. More precisely, this diffuseness is commonly believed to be caused by point, line, or planar defects or even strain-gradiants existing inside the films.[16–20] However, Ref. 21 recently suggested another origin, namely, that such diffuseness is a manifestation of strain-induced or surface-induced *dipolar disorder*.

The aim of this paper is to use a first-principles-derived technique to reveal the origin of the diffuse character of the paraelectric-to-ferroelectric phase transition in ferroelectric ultrathin films and to determine the precise effect of electrical and mechanical boundary conditions, as well as the film's thickness, on such diffuseness. One important finding is that the existence of such diffuseness does not require the presence of defects. We rather discovered that surface-induced dipolar inhomogeneities between different film's layers (rather than a dipolar disorder within the film) can lead to such diffuseness.

This paper is organized as follows. Section II describes the numerical method we used. Section III presents our computation results and discusses them in details. Finally, Sec. IV briefly summarizes our findings.

II. METHODS

In this work, we simulate *defect-free* thin films made of $BaTiO_3$ (BT), that are grown along the [001] pseudocubic direction (chosen to be along the z axis) and are Ba-O terminated at all surfaces/interfaces. These films are modeled by $L\times L\times m$ supercells that are periodic along the x and y axes (which lie along the [100] and [010] directions, respectively) and contain m (001) TiO_2 layers stacked along the *finite* z axis. Here, we chose to generalize the first-principles-derived scheme of Ref. 23—that has been initially developed for $Ba_{1-x}Sr_xTiO_3$ (BST) *bulks* with any composition—to $BaTiO_3$ thin films, because it provides critical temperatures of BT bulk in good agreement with measurements. The generalization to BST *thin films* (for any Ba concentration, including 100%) consists in writing their total energies, $\mathcal{E}_{tot}$, as

$$\mathcal{E}_{tot}(\{\mathbf{u_i}\},\eta_H,\{\mathbf{v}_i\},\{\sigma_i\},\{\eta_{loc}\}) = \mathcal{E}_{Heff}(\{\mathbf{u_i}\},\eta_H,\{\mathbf{v}_i\},\{\sigma_i\},\{\eta_{loc}\}) + \frac{1}{2}\beta\sum_i \langle\mathbf{E}_{dep}\rangle\cdot Z^*\mathbf{u_i}, \quad (1)$$

where $\mathbf{u_i}$ is the displacement of the Ti-centered local soft modes in the unit cell i of the film ($Z^*\mathbf{u_i}$ yields the local electrical dipole in that unit cell, with Z^* being a Born effective charge[24]). η_H is the homogeneous strain tensor, while $\mathbf{v}_i$ are inhomogeneous strain-related variables.[24] $\{\sigma_i\}$ characterizes the alloying configuration and $\{\eta_{loc}\}$ is the strain arising

from the difference in size between Ba and Sr ions.[23] $\mathcal{E}_{Heff}$ represents the intrinsic (effective Hamiltonian) energy of the BST films. The first-principles-derived parameters and analytical expression of $\mathcal{E}_{Heff}$ are those given in Ref. 23 for bulk BST except for the dipole-dipole interactions for which we use here the formula derived in Ref. 25 for thin films under ideal *open-circuit* (OC) conditions. Such electrical boundary conditions naturally lead to the existence of a maximum depolarizing field (denoted by $\langle \mathbf{E}_{dep} \rangle$ and self-consistently determined from the atomistic approach of Ref. 25) inside the film. The second term of Eq. (1) mimics a screening of $\langle \mathbf{E}_{dep} \rangle$ via the β parameter. $\beta=0$ corresponds to ideal OC conditions, while an increase in β lowers the magnitude of the resulting depolarizing field, and $\beta=1$ corresponds to ideal short-circuit (SC) conditions for which the depolarizing field has vanished (note that the existence of dead/passive layers at the electrode-film interface can be thought as corresponding to small β values[26]). Moreover, mechanical boundary conditions associated with *epitaxial* (001) films can also be mimicked by freezing some components of the homogeneous strain tensor.[9,27] On the other hand, *stress-free* systems are simulated by allowing the relaxation of *all* the components of the strain tensor. Technically, $\mathcal{E}_{tot}$ is used in two different kinds of Monte Carlo (MC) simulations. The first kind involves the Metropolis algorithm,[28] while the second kind of MC simulations is conducted within the so-called Wang-Landau algorithm.[29] The Metropolis algorithm is used here to extract the layer-by-layer decomposition of the local soft modes at any temperature (since extracting local configurations is not trivial within the Wang-Landau algorithm). Moreover, the use of the Wang-Landau technique allows here a "smooth" computation of the thermal average of the supercell average of the local modes, $\langle \mathbf{u} \rangle$, (that is directly proportional to the electrical polarization) and of the dielectric susceptibility, χ_{33} (where the "3" index refers to the z axis), for each temperature, T. In other word, one strength of this Wang-Landau algorithm is to provide these latter quantities with no large fluctuations for any temperature (unlike the Metropolis algorithm[28] that usually yields relatively large fluctuations of the physical properties close to the transition temperature). Note also that the Wang-Landau approach is based on the observation that if configurations c with total energy $E(c)$ are sampled with a probability proportional to the reciprocal of the density of states $1/g[E(c)]$, then the resulting energy histogram is flat. The goal of the Wang-Landau algorithm is to determine the density of state, $g(E)$. Such determination is accomplished via a random walk in the energy space (with this space being practically divided into several energy bins E_i) with a probability proportional to $1/g(E)$. The density of states and the energy histograms, $H(E_i)$, are both updated each time an energy bin E_i is visited. The fact that the probability of the random walk is proportional to $1/g(E)$ naturally guarantees that the energy histogram becomes flat when all energy bins are about equally well sampled (as they should be when reaching convergency). One particular strength of the Wang-Landau algorithm is that many thermodynamics quantities can be precisely computed for any temperature, once having solely determined $g(E)$. In our simulations, the energy histograms are typically checked every 25×10^4 Monte Carlo (MC) sweeps, and we impose the $H(E_i)$ of the lowest energy bin to be larger than 80% of the value of the energy histogram averaged over all energy bins (as our criterion of flatness). More details of the Wang-Landau algorithm can be found in Refs. 29.

The quantification of the diffuseness of the phase transition (if any) is practically accomplished by fitting the predicted χ_{33} (in the paraelectric phase) by the Martinera and Burfoot equation,[30]

$$\frac{1}{\chi_{33}} - \frac{1}{\chi_{33,\max}} = C(T - T_c)^{\gamma}, \tag{2}$$

where T_c is the temperature at which the dielectric response is maximum, and where $\chi_{33,\max}$, γ and C are determined from the fit. For the present study, γ is the most important parameter since it provides information about the diffuseness of the phase transition: for $\gamma=1$, the transition is of the Curie-Weiss type, while the transition is considered to be a complete diffuse phase transition when $\gamma=2$.[30] A value-in-between for γ thus corresponds to an intermediate situation between these two limiting cases.

III. RESULTS

Figure 1(a) displays the predicted thermal average of the magnitude of the z component of the supercell average of the local mode vector, $\langle |u_z| \rangle$, for a *stress-free* BT thin film having a thickness of 24 Å and being under ideal SC conditions—as mimicked by a $12\times12\times6$ supercell with the β parameter of Eq. (1) being equal to 1—as a function of T-T_c.[31] $\langle |u_z| \rangle$ increases from rather small to more significant values when decreasing the temperature below the T_c critical temperature, which indicates that this BT film undergoes a phase transition from a paraelectric cubic phase to a tetragonal ferroelectric structure having a polarization oriented along the z axis. Interestingly, Fig. 1(a) already hints that this transition is diffuse in nature because of the significant polarization's tail occurring above T_c. Moreover, Fig. 1(b) reveals that χ_{33} of this 24 Å thick, stress-free BT film is rather broad with respect to temperature. This confirms the *diffuse* character of that phase transition, as consistent with measurements[11–21] and as evidenced by Table I that reports a predicted γ parameter around 1.59.

It is important to realize that the smear of the dielectric anomaly with film thickness has been experimentally found to start occurring near 40–1000 nm,[14,15,21] while the smear of polarization usually takes place at 10 nm or less. Saad *et al.* called the former as a "dynamic" size effect, while the latter is denoted as a "static" size effect.[32] Here, we can only study the static size effect because modeling films with a thickness of 40–1000 nm is beyond our present computational possibilities. Such static size effect is clearly evidenced in Figs. 1(a) and 1(b), where the smear of the polarization and dielectric response can both be seen.

Note that Figs. 1(a) and 1(b) also present $\langle |u_z| \rangle$ and χ_{33} for BT *bulk*, as mimicked by a $12\times12\times12$ supercell that is periodic along any of the three Cartesian directions.[33] One can see two jumps of $\langle |u_z| \rangle$ below T_c, that coincide with the well-known tetragonal–to-orthorhombic and orthorhombic-

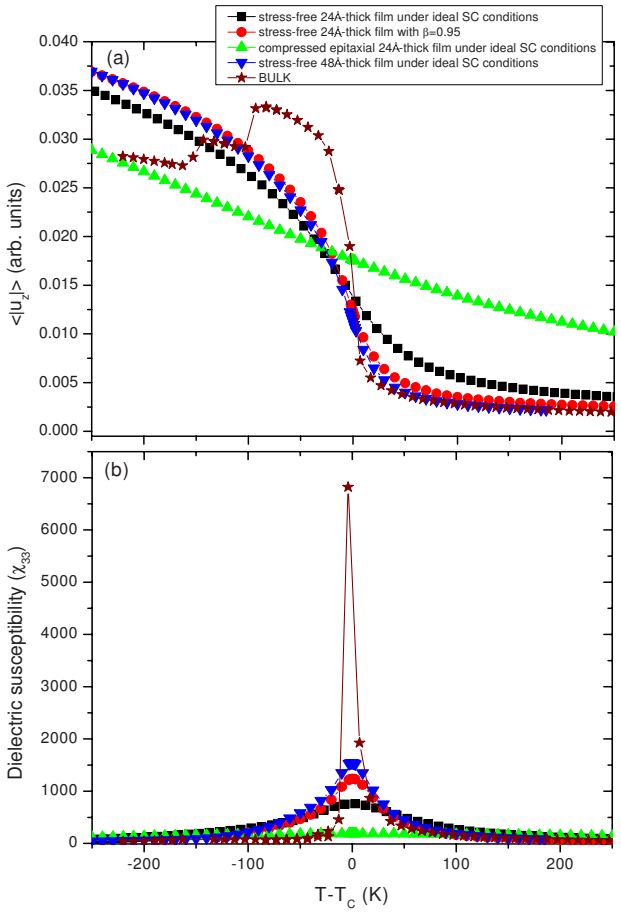

FIG. 1. (Color online) Thermal average of the magnitude of the z component of the supercell average of the local mode vector [$\langle|u_z|\rangle$, panel (a)] and of the out-of-plane dielectric susceptibility [χ_{33}, panel (b)] as a function of the reduced temperature (T-T_c), in the studied (001) BT ultrathin films. T_c is the temperature at which χ_{33} peaks. The other (x and y) components of the local mode are not shown in panel (a) because they are nearly null for the displayed temperatures. The corresponding data for BT bulk are also indicated.

to-rhombohedral transitions of BT bulk, respectively.[23,35] Furthermore, the corresponding γ parameter of BT bulk is numerically found to be around 1.05, according to our Wang-Landau simulations, that is very close to the ideal Curie-Weiss value of 1 as well as to the value of 1.08 experimentally reported in Ref. 36 for BT bulk.

Figures 1(a) and 1(b) also show $\langle|u_z|\rangle$ and χ_{33} of three other BT thin films, as a function of their own reduced temperature, T-T_c.[37] Their differences with respect to the previously studied film stem either from the electrical boundary conditions (namely, the β parameter is now chosen to be 0.95 rather than 1), the mechanical boundary conditions (by considering a BT film under a compressive, epitaxial strain of −2%, rather than being under stress-free conditions), or the film's thickness (by selecting m=12 rather than 6). As indicated in Table I, the critical temperature is dramatically affected by such differences.[38] For instance, T_c decreases when decreasing the β parameter, as consistent with the fact that an increase in magnitude of the depolarizing field tends to suppress the spontaneous polarization.[7] On the other hand, the compressive epitaxial strain strongly increases the critical temperature of BT films, as consistent with previous findings of Refs. 6, 11, and 39. Note also that, as revealed by Fig. 1(a), all the studied films exhibit a net polarization along the z axis below their T_c critical temperature[35] (domains with no net polarization arise for values of β smaller than those investigated here, along with large enough compressive strain[9]). Table I reports the corresponding γ parameters arising from the fit of the dielectric response displayed in Fig. 1(b) by Eq. (2) for all the presently considered cases. Regarding the effect of electrical boundary conditions on physical properties, the most notable observation is that decreasing β from 1 to 0.95 in the stress-free, 24 Å thick BT film reduces the polarization tail and makes the dielectric response less broad, resulting in a dramatic decrease in γ from 1.59 to 1.23. In other words, our calculations reveal that "slightly" increasing the magnitude of the depolarizing field results in a less diffuse phase transition. On the other hand, going from a stress-free mechanical boundary condition to a compressive strain in the 24 Å thick BT film, while keeping it under ideal SC conditions, generates a polarization tail that is still significant for temperature much above T_c [see Fig. 1(a)] and a γ parameter that increases up to 1.71. Such findings are consistent with the observations of Ref. 11 that the epitaxial strain arising from the substrate increases the diffuseness of the paraelectric-to-ferroelectric phase transition in ferroelectric thin films. Finally, Fig. 1 and Table I indicate that such transition becomes less diffuse when solely increas-

TABLE I. Critical temperature and parameters quantifying the diffuse character of the paraelectric-to-ferroelectric transition [γ, see Eq. (2)] and the dipoles' inhomogeneity [g_z, see Eq. (3)] in the presently studied (001) BT ultrathin films. We numerically checked the convergency of our results with respect to the periodic in-plane supercell length, L, by typically considering three different values for L (namely, L=12, 18, and 24). T_c is given in Kelvins, γ is dimensionless, and g_z is given, in lattice constant units, at the fixed small temperature of 50 K and at the fixed T/T_c ratio of 0.9. The predicted T_c is close to 390 K in BT bulk, in good agreement with experiments (Ref. 23).

Studied BT film	T_c (K)	γ	$g_z(T=50\ \text{K})$	$g_z(T/T_c=0.9)$
Stress-free, 24 Å thick, under SC conditions	1357	1.59	0.093	0.030
Stress-free, 24 Å thick, with β=0.95	667	1.23	0.051	0.024
Compressed, 24 Å thick, under SC conditions	2155	1.71	0.103	0.031
Stress-free, 48 Å thick, under SC conditions	855	1.55	0.079	0.025

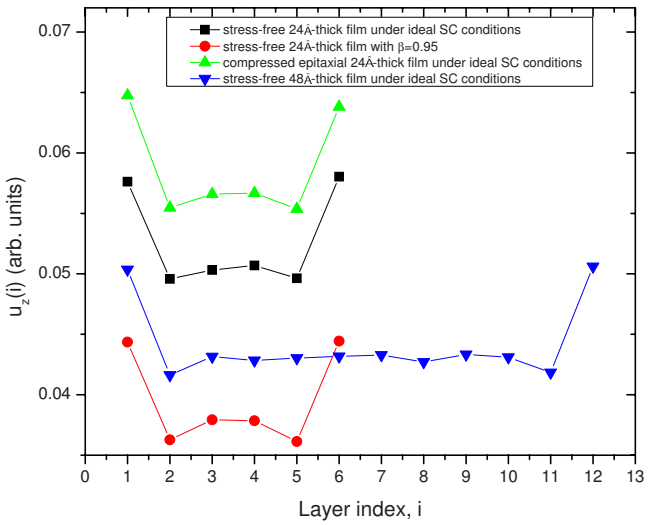

FIG. 2. (Color online) Local ferroelectric distortions along the z axis as a function of the layer index along the growth direction, at 50 K, in the presently studied (001) BT ultrathin films. The minimal and maximal indices characterize the TiO_2 layers that are closest to the surfaces/interfaces.

ing the film's thickness, as evidenced by, e.g., the decrease in γ from 1.59 to 1.55 when increasing m from 6 to 12 in a stress-free BT film under ideal SC conditions. Such trend is consistent with the measurements of Ref. 13 that observed a decrease in γ from 1.98 to 1.78 when increasing the thickness from 50 to 320 nm in BT thin films (note that such grown films likely have defects and the aforementioned dynamic size effect, which can contribute to the reported large values of γ).

Having established that our scheme can reproduce the diffuse character of the phase transition in ferroelectric thin films, let us determine the microscopic origin of our findings. For that, Fig. 2 reports the layer-by-layer decomposition of the thermal average of the z component of the supercell average of the local mode vector, $\langle u_z \rangle$, for all our considered BT films, at 50 K. One can clearly see a rather large *surface-induced inhomogeneity* of the dipoles. More precisely, the layers being the closest to the surface/interfaces exhibit a $\simeq$15% enhancement of their magnitude with respect to the dipoles centered in the inner layers. Such enhancement has been previously reported in several low-dimensional systems,[7,40–42] and arises from the truncation of short-range interactions—that oppose the onset of local dipoles, near the surfaces/interfaces.[43] The quantification of such dipoles' inhomogeneity can be practically done by computing

$$g_z = \sqrt{\frac{1}{N}\sum_i [u_z(i) - \langle u_z \rangle]^2}, \tag{3}$$

where the sum over the i index runs over all the different m (001)-TiO_2 layers and where $u_z(i)$ is the z component of the local mode *averaged in the layer i* (while $\langle u_z \rangle$ is the z component of the local mode averaged over the whole film, as indicated above). Table I provides the values of g_z at the fixed small temperature of 50 K, as well as at the fixed T/T_c ratio of 0.9, in all four studied cases (note that T_c varies between these different cases, as indicated in Table I). Table I reveals a well-definite correlation between these g_z and the "diffuse" γ parameter: the larger g_z the bigger γ. In other words, our calculations demonstrate that the diffuse character of the phase transition originates from surface-induced dipolar inhomogeneities. Figure 2 and Table I also provide the microscopic reason for the reduction in the diffuse character of the phase transition when decreasing β: it simply arises from the fact that the difference between the local dipoles at the surfaces and those inside the film decreases as the magnitude of the depolarizing field increases. Conversely, such difference increases when going from stress-free mechanical boundary conditions to a significant value of the compressive epitaxial strain, which thus results in a larger g_z and thus to a more diffuse phase transition. Finally, increasing the film's thickness leads to a reduction in the overall inhomogeneity and therefore to a less diffuse phase transition, because of the resulting decrease in the ratio between the dipoles centered at the surface layers and those located in the inner layers.

IV. SUMMARY AND DISCUSSION

In summary, our first-principles-based effective Hamiltonian calculations indicated that the paraelectric-to-ferroelectric phase transition of ultrathin films can have a diffuse character even in defect-free films. Such diffuseness is found to originate from surface-induced dipolar inhomogeneities. It naturally depends on the mechanical and electrical boundary conditions and film's thickness because such films' characteristics affect the difference between surface and inner dipoles.

Note that recent first-principles calculations showed that the surface-induced *enhancement* of dipoles shown in Fig. 2 may not be a systematic property of electroded $BaTiO_3$ films, and may, in fact, depend on the chemical nature of the electrode (e.g., $SrRuO_3$ versus Pt).[44] Interestingly, Eq. (3) and its aforementioned connection to the γ parameter suggest that what matters for the occurrence of diffuse phase transition is the *difference* between surface/interface and inner dipoles. In other words, it is likely that an electrode causing the dipoles at the surface/interface to be smaller than those inside the films will still yield a diffuse phase transition, providing that the difference between these two types of dipoles is significant enough. We thus hope that our study will deepen the current understanding of phase transition in low-dimensional dipolar systems.

ACKNOWLEDGMENTS

This work is supported by ONR Grants No. N00014-04-1-0413, No. N00014-08-1-0915, and No. N00014-07-1-0825 (DURIP), and NSF Grants No. DMR 0701558, No. DMR-0404335, and No. DMR-0080054 (C-SPIN), and by DOE grant DE-SC0002220. Some computations were made possible thanks to MRI Grant No. 0722625 from NSF and to a Challenge grant from HPCMO of the U.S. Department of Defense. We thank B. Dkhil for useful discussions.

[1] J. F. Scott, J. Phys.: Condens. Matter **18**, R361 (2006).
[2] I. Kornev, H. Fu, and L. Bellaiche, J. Mater. Sci. **41**, 137 (2006).
[3] M. Dawber, K. M. Rabe, and J. F. Scott, Rev. Mod. Phys. **77**, 1083 (2005).
[4] J. F. Scott, *Ferroelectric Memories* (Spring-Verlag, Berlin, 2000).
[5] J. Junquera and P. Ghosez, Nature (London) **422**, 506 (2003).
[6] D. G. Schlom, L.-Q. Chen, C.-B. Eom, K. M. Rabe, S. K. Streiffer, and J.-M. Triscone, Annu. Rev. Mater. Res. **37**, 589 (2007).
[7] B.-K. Lai, I. A. Kornev, L. Bellaiche, and G. J. Salamo, Appl. Phys. Lett. **86**, 132904 (2005).
[8] S. K. Streiffer, J. A. Eastman, D. D. Fong, Carol Thompson, A. Munkholm, M. V. Ramana Murty, O. Auciello, G. R. Bai, and G. B. Stephenson, Phys. Rev. Lett. **89**, 067601 (2002).
[9] I. Kornev, H. Fu, and L. Bellaiche, Phys. Rev. Lett. **93**, 196104 (2004).
[10] B.-K. Lai, I. Ponomareva, I. I. Naumov, I. Kornev, H. Fu, L. Bellaiche, and G. J. Salamo, Phys. Rev. Lett. **96**, 137602 (2006).
[11] B. Dkhil, E. Defay, and J. Guillan, Appl. Phys. Lett. **90**, 022908 (2007).
[12] A. K. Tagantsev, N. A. Pertsev, P. Muralt, and N. Setter, Phys. Rev. B **65**, 012104 (2001).
[13] S. Chattopadhyay, A. R. Teren, J. H. Hwang, T. O. Mason, and B. W. Wessels, J. Mater. Res. **17**, 669 (2002).
[14] K. R. Udayakumar, P. J. Schuele, J. Chen, S. B. Krupanidhi, and L. E. Cross, J. Appl. Phys. **77**, 3981 (1995).
[15] Y. Sakashita, H. Segawa, K. Tominaga, and M. Okada, J. Appl. Phys. **73**, 7857 (1993).
[16] Z. Surowiak, A. M. Margolin, I. N. Zakharchenko, and S. V. Biryukov, Thin Solid Films **176**, 227 (1989).
[17] V. S. Tiwari, N. Singh, and D. Pandey, J. Phys.: Condens. Matter **7**, 1441 (1995).
[18] Y. Fukuda, K. Numata, K. Aoki, and A. Nishimura, Jpn. J. Appl. Phys., Part 1 **35**, 5178 (1996).
[19] L. W. Chang, M. McMillen, and J. M. Gregg, Appl. Phys. Lett. **94**, 212905 (2009).
[20] G. Catalan, B. Noheda, J. McAneney, L. J. Sinnamon, and J. M. Gregg, Phys. Rev. B **72**, 020102(R) (2005).
[21] M. Tyunina, J. Levoska, and I. Jaakola, Phys. Rev. B **75**, 140102(R) (2007).
[22] L. E. Cross, Ferroelectrics **151**, 305 (1994).
[23] L. Walizer, S. Lisenkov, and L. Bellaiche, Phys. Rev. B **73**, 144105 (2006).
[24] W. Zhong, D. Vanderbilt, and K. M. Rabe, Phys. Rev. Lett. **73**, 1861 (1994); Phys. Rev. B **52**, 6301 (1995).
[25] I. Ponomareva, I. I. Naumov, I. Kornev, H. Fu, and L. Bellaiche, Phys. Rev. B **72**, 140102(R) (2005); I. Naumov and H. Fu, arXiv:cond-mat/0505497 (unpublished).
[26] S. Prosandeev and L. Bellaiche, Phys. Rev. B **75**, 172109 (2007).
[27] N. A. Pertsev, V. G. Kukhar, H. Kohlstedt, and R. Waser, Phys. Rev. B **67**, 054107 (2003).
[28] N. Metropolis, A. W. Rosenbluth, M. N. Rosenbluth, A. H. Teller, and E. Teller, J. Chem. Phys. **21**, 1087 (1953).
[29] F. Wang and D. P. Landau, Phys. Rev. Lett. **86**, 2050 (2001); Phys. Rev. E **64**, 056101 (2001).
[30] B. E. Vugmeister and M. D. Glinichuk, Rev. Mod. Phys. **62**, 993 (1990); O. G. Vendik and L. T. Ter-Martirosyan, J. Appl. Phys. **87**, 1435 (2000).
[31] The probability of having the z component of the polarization being positive is exactly equal to the probability of having the z component of the polarization being negative, below T_c. As a result, the Wang-Landau algorithm will predict a *null* value for the thermal average of the z component of the supercell average of the local mode vector [unlike the Metropolis algorithm (Ref. 28) that breaks such symmetry]. That is why we calculate $\langle|u_z|\rangle$, and not $\langle u_z\rangle$, within the Wang-Landau algorithm.
[32] M. M. Saad, P. Baxter, J. McAneney, A. Lookman, L. J. Sinnamon, P. Evans, A. Schilling, T. Adams, X. Zhu, R. J. Pollard, R. M. Bowman, J. M. Gregg, D. J. Jung, F. D. Morrison, and J. F. Scott, IEEE Trans. Ultrason. Ferroelectr. Freq. Control **53**, 2208 (2006).
[33] Note that the fact that $\langle|u_z|\rangle$ of $BaTiO_3$ bulk is not exactly zero above T_c arises from size effects associated with the finite lengths of the supercell used to mimic $BaTiO_3$ bulk (see, e.g., Ref. 34).
[34] K. Binder, Rep. Prog. Phys. **60**, 487 (1997).
[35] Note that all the ultrathin films studied here only exhibit a paraelectric-to-tetragonal phase transition, that is no ferroelectric orthorhombic and rhombohedral phases are found here, because of the small investigated film's thicknesses and boundary conditions.
[36] G. A. Samara, Phys. Rev. **151**, 378 (1966).
[37] Note that all the BT ultrathin films investigated here are numerically found to exhibit a *second-order* paraelectric-to-ferroelectric phase transition (unlike the corresponding bulk), as consistent with measurements (Ref. 19).
[38] Note that films with T_c larger than $\simeq$1920 K are not expected to be in their solid phase, since such latter temperature corresponds to the melting point of $BaTiO_3$. We nevertheless reported such large values in Table I to "simply" indicate the general trend of the critical temperature of $BaTiO_3$ films with electrical and mechanical boundary conditions, as well as, with thickness.
[39] S. Bin-Omran, I. Ponomareva, and L. Bellaiche, Phys. Rev. B **77**, 144105 (2008).
[40] P. Ghosez and K. M. Rabe, Appl. Phys. Lett. **76**, 2767 (2000).
[41] J. E. Spanier, A. Kolpak, I. Grinberg, J. J. Urban, L. Ouyang, W. S. Yun, A. M. Rappe, and H. Park, Nano Lett. **6**, 735 (2006).
[42] N. Sai, A. M. Kolpak, and A. M. Rappe, Phys. Rev. B **72**, 020101(R) (2005).
[43] Figure 2 indicates that decreasing β leads to a smaller $\langle u_z\rangle$ at a fixed low temperature, which arises from the fact that it corresponds to increasing the magnitude of the depolarizing field (that opposes the formation of the out-of-plane component of the polarization) (Refs. 5, 7, and 39). One can also note from Fig. 2 that the coupling between local dipoles and strain results in an enhancement of the z component of the polarization of BT films (at a fixed low temperature) by the compressive strain, as consistent with previous works (see, e.g., Refs. 7, 9, and 39, and references therein). Moreover, $\langle u_z\rangle$ is numerically found to decrease, at a fixed low temperature, when increasing the film's thickness because of the fact that the ratio between surface layers (which exhibit the largest value for the z component of the dipoles, see Fig. 2) and inner layers decreases as the film's thickness increases (Refs. 7 and 39). The fact that $\langle|u_z|\rangle$ for the stress-free 24 Å thick film under ideal SC conditions is below the lines of the rest of the considered cases for temperatures lower than T_c in Fig. 1 while $\langle u_z\rangle$ has the largest value in Fig. 2 stems from the

facts that (i) its T_c is the largest among all cases considered here; (ii) its phase transition is the more diffuse one (i.e., its γ parameter is the largest); and (iii) that the horizontal axis of Fig. 1 is the reduced temperature (i.e., T-T_c), while the data of Fig. 2 correspond to a fixed low temperature (namely, 50 K). Note that $\langle u_z \rangle$ is positive in Fig. 2 [i.e., the z component of the polarization is found positive here within the Metropolis algorithm (Ref. 28)], which thus makes it equal to $\langle |u_z| \rangle$ and thus allows the comparison between Fig. 1(a) (whose results are from the use of the Wang-Landau algorithm [Ref. 29)] and Fig. 2 [whose data arise from the use of the Metropolis algorithm (Ref. 28).

[44] M. Stengel, D. Vanderbilt, and N. A. Spaldin, Phys. Rev. B **80**, 224110 (2009).